

THE THESAURUS PROJECT, A LONG RANGE AUV FOR EXTENDED EXPLORATION, SURVEILLANCE AND MONITORING OF ARCHAEOLOGICAL SITES

B.ALLOTTA†, L.PUGI†, F.BARTOLINI†, R.COSTANZI†, A.RIDOLFI†, N.MONNI†, J.GELLI†, G.VETTORI†, L.GUALDESI°, M.NATALINI†

†MDM Lab, Industrial Engineering Department

University of Florence

via Panconi 12, Pistoia, Italy

e-mail: luca.pugi@unifi.it, <http://www.unifi.it/mdmlab>

°Edgelab SRL www.edgelab.eu

Keywords: Autonomous Underwater Vehicle, Design Optimization, Swarm Control and Navigation

Abstract.

Within the framework of the Thesaurus project (Italian acronym for “Tecniche per l’Esplorazione Sottomarina Archeologica mediante l’Utilizzo di Robot autonomi in Sciame”), the authors have developed a low cost, multirole Autonomous Underwater Vehicle, briefly called Tifone, whose design is the main topic of this paper. According to the expected performances and specifications, the vehicle has to maintain a good autonomy and efficiency, typical features of an AUV (Autonomous Underwater Vehicle), also maintaining high manoeuvrability and hovering capabilities, which are instead more common on ROVs (Remotely Operated Vehicles). Cooperative exploration and surveillance tasks involve the use of swarms of vehicles; the control, the mutual localization and communications among vehicles are fundamental tasks to be optimized. In particular, the optimization of costs with respect to benefits plays a critical role, considering that within the Thesaurus project a first fleet of three vehicles has to be developed. This work mainly deals with the different design phases of the vehicle and with the results of preliminary simulations and tests performed in the MDM laboratories, before the next lake (Roffia basin, between Pisa and Florence, Italy) and sea testing activities (Elba Island, Italy) that will be performed in spring and summer 2013.

1 INTRODUCTION: THESAURUS PROJECT AND VEHICLE SPECIFICATIONS.

Aim of the Thesaurus project is the development of a swarm of AUVs (Autonomous Underwater Vehicles) for the exploration, surveillance and monitoring of archaeological sites. The swarm is composed of 3 identical vehicles, briefly called Tifone, that can be customized to perform different tasks/roles assigned in a cooperative mission profile, including acoustic or visual inspection of the site of interest. In particular, a feasible composition of the swarm

with three different vehicle layouts, corresponding to different mission tasks and instrumentation layouts, is visible in Figure 1:

- Acoustic Explorer: this vehicle is equipped with long/medium range instrumentation, such as Side Scan Sonar (SSS), in order to explore and investigate relatively wide areas, for a large, medium scale reconstruction of the site or a preliminary exploration of a potentially interesting area. The typical distance from a potential target on the sea-bottom is 40 m or more;
- Vision Explorer: this is the vehicle equipped with short range instrumentation, like cameras, illuminators and/or structured lights, for visual inspection and monitoring of a site. Its applications can be the 3D reconstruction for virtual reality or augmented reality applications, or more ambitiously, a visual based SLAM (Simultaneous Localization And Mapping) of the site. The typical distance from a potential target is about 4 m;
- Swarm Coordinator: the communication and the mutual localization of the swarm AUVs is performed by the Swarm-Coordinator through an USBL (Ultra-Short BaseLine) system. The coordinator is equipped with a transceiver; on the other vehicles the acoustic modems, working as transponders, are installed. The estimation of the absolute position of the coordinator should be periodically fixed using its GPS signal, which implies the periodical emersion of the vehicle. In this way, the swarm coordinator can communicate with the on-board navigation system of each vehicle, to refine the mutual position estimation and to perform the cooperative localization of the whole swarm. Some preliminary simulations concerning possible strategies to be used to perform the mutual localization of the vehicles have been the object of a previous publication [1].

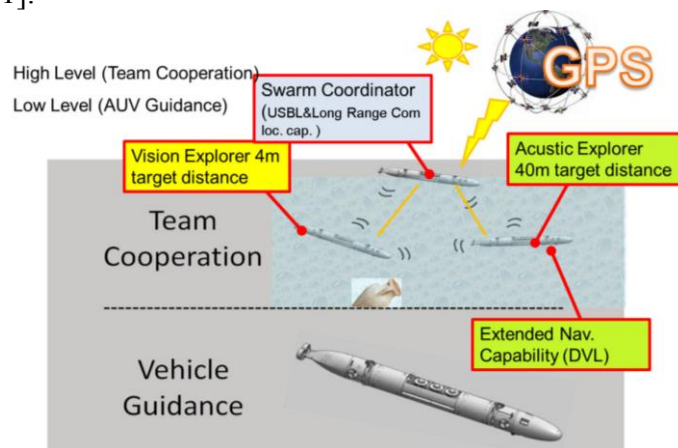


Figure 1: Typical swarm configuration and different vehicle layouts

The vehicle technical specifications were decided considering the performances of existing AUV and in particular with respect to [7], Tifone specifications involve the capability of exploring extended areas, with an autonomy of more than 12 hours with a cruise and a peak speed of respectively 3-4 and 6-7 knots (corresponding to an estimated travelled distance between 150 and 200 km). The maximum operating depth is about 300 m (plus a 20% of safety margin). Good Maneuverability and hovering capabilities are also mandatory specifications, considering the possibility of performing complex cooperative tasks over the

investigated site, including acoustic inspection and visual recognition. An on-board payload of more than 20 kg of instruments have been considered in the design of the vehicle. Optional-future development will consider the feasibility of external payload, such as a manipulating devices, different kind of sensors or, moreover, micro AUV or ROV can be transported on the mission site by Tifone.

2 ON-BOARD EQUIPMENT AND PAYLOAD

Since every vehicle can be customized to manage different payloads and mission profiles the system was designed by dividing the on-board subsystems in two main categories, as shown in Figure 2 and Figure 4:

- **Vital Systems:** all the navigation, communication and safety related components and functions of the vehicle are controlled by a rugged industrial PC-104 called Vital PC, whose functionality is continuously monitored by a watchdog system. All the components corresponding to vital functions common to all the Tifone vehicles are directly controlled by the Vital PC. Most of the code implemented on the Vital PC, and consequently the corresponding computational load, is quite invariant with respect to the mission profiles and payloads, assuring a high stability of the system also considering the wide variability of operating conditions.
- **Customizable Payloads:** all the additional functions related to variable payloads are controlled by one or more Data PC to which all the additional sensors and subsystem are connected. In particular, the Data PC also manages the storage on mass memories (conventional hard discs or solid state memories) and the data coming from the connected sensors. In this way, all the processes introduced by additional payloads are implemented on a platform which is also physically separated from the vital one, and also from an electrical point of view the two parts are protected independently through fuses and relays.

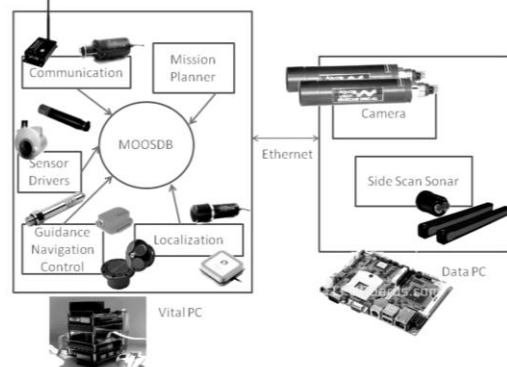


Figure 2: Division between Vital instruments installed on the Vital PC and optional payloads controlled by the Data PC

The on-board integration utilizes MOOS [3] (Mission Oriented Operating Suite) as software infrastructure. MOOS is a publish/subscribe system for inter-process communication (IPC), which supports dynamic, asynchronous, and distributed communication. Its basic functioning, usual in all pub/sub systems, relies on a dispatcher, which is responsible for routing messages from publishers to subscribers. The messages are routed based on their topics, which is an information descriptor contained in the messages themselves. In the case of MOOS the dispatcher is represented by a central database (MOOSDB), which is hence responsible to route the information according to the client registrations, as shown in Figure 3. According to

this paradigm, each process on-board the vehicle will hence be represented by a MOOS client connected to the central database. The main advantage of the chosen software architecture is the easiness of implementing system with distributed intelligence, in which more than one Data PC is used to manage future/optional payloads which have not been taken into account within the original design of the system.

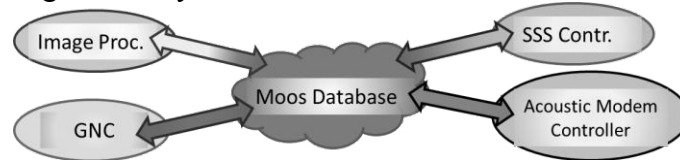


Figure 3: MOOS concept, all the processing (for instance, GNC=Guidance and Navigation Control) on-board the vehicle connect to the central database which is responsible to route the information according to their registrations

In Figure 4, a simplified scheme of the electric plant is shown: considering the size of the vehicle, including the foreseen propulsion system, a 48V DC bus was chosen for both propulsion and energy storage system. To feed other instruments and sensors 24V DC, 15V DC and 12V DC voltages are provided by suitable DC-DC converters.

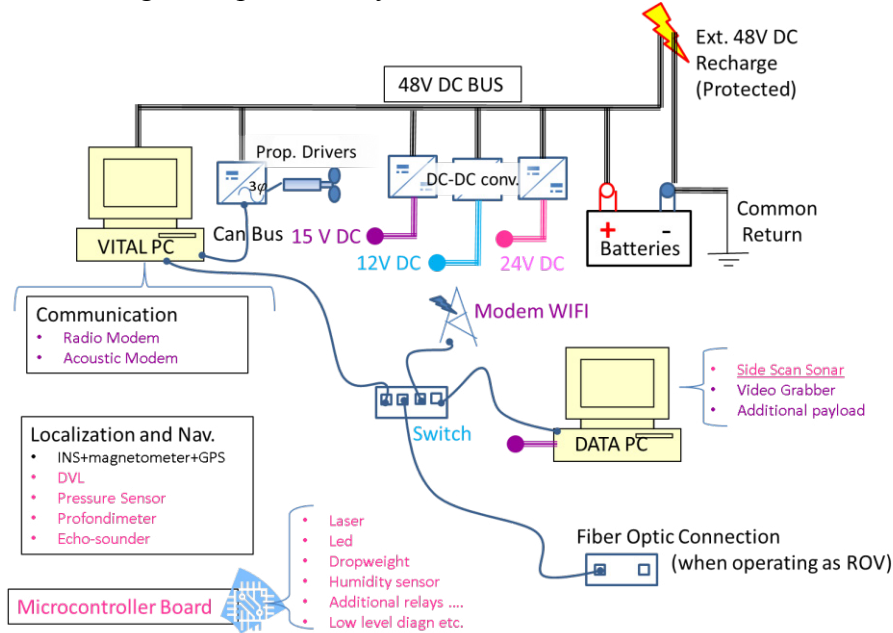


Figure 4: Simplified electric/functional scheme of the plant

2 PRELIMINARY VEHICLE AND SIMULATION MODEL DESCRIPTION

In order to properly size both the propellers and the energy storage system, the dynamical behaviour of the vehicle was reproduced using the approach proposed by [4] which is briefly described by (1):

$$M\dot{v} + C(v)v + D(v)v + g(\eta) = \tau \quad (1)$$

where vectors τ , η , v are defined according to Table 1 and the reference system described in Figure 5, matrices M , C , D are introduced to model the contributions of the inertial,

Coriolis and viscous effects [8], while vector g represents the combined effects of gravity W and buoyancy B .

Table 1: Reference system (body constrained) and corresponding kinematical/dynamical variables

Degree of freedom	Corresponding Motion	Forces, Torques(τ)	Speed (ν)	Pos.Ang. Coordinates (η)
1	Surge (linear motion along x axis)	X	u	x
2	Sway (linear motion along y axis)	Y	v	y
3	Heave (linear motion along z axis)	Z	w	z
4	Roll (rotation along body x axis)	K	p	ϕ
5	Pitch (rotation along body y axis)	M	q	θ
6	Yaw (rotation along body z axis)	N	r	ψ

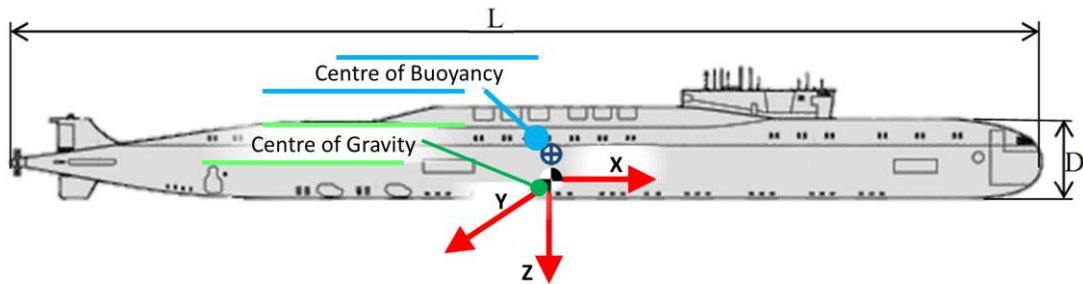


Figure 5: Definition of the body reference system, centres of Buoyancy and Gravity

The values of the coefficients in (1) have been extrapolated considering the results of previous CFD simulations and the know-how available in literature [4],[5],[6],[7].

The calculation of τ is performed considering the layout of the propulsion system which is composed by six actuators: two rear propellers, two lateral and two vertical manoeuvring thrusters (as shown in Figure 6) are used to control 5 DOFs (degrees of freedom) of the vehicle, the three linear translations along x,y,z (surge, sway and heave) and the yaw and pitch rotations. In Table 2 some of the most significant features of the vehicle are also shown.

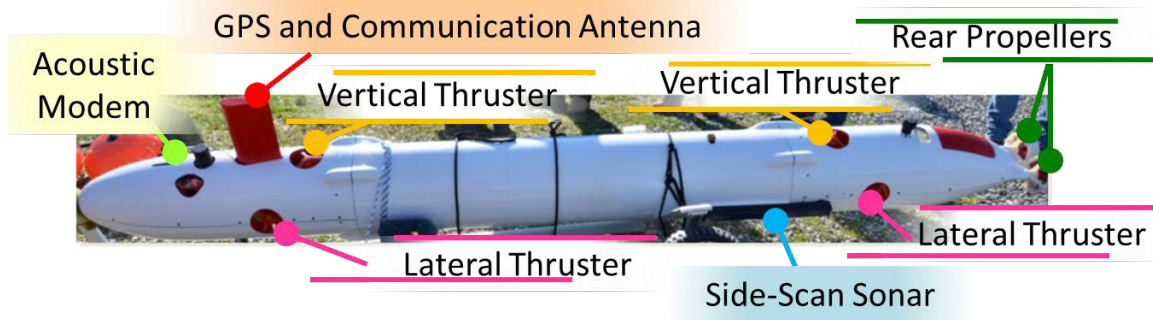


Figure 6: Layout and main components of the Tifone vehicle

Table 2: Main features of Tifone Vehicle

Dimensions (L,D)	Weight in Air /Volume	Speed (cruise, max)	Autonomy (time, trav.distance)	Max Operating Depth
(3.5m, 320mm)	160kg/240dm ³	(2m/s, 3.5-4m/s)	(8-12h, 150-200km)	300m (60m of safety margin)

The propulsion layout, described in Figure 6, is common to some known hybrid glider solutions, such as the italian Folaga [9]. Knowing the six thrusts T_i (i indicates the i -th propeller), vector τ is calculated through a constant coefficient matrix R easily evaluated considering static balance considerations (2).

$$\tau = RT; \tag{2}$$

where T is a vector whose scalar components are the efforts T_i exerted by the actuators

The thrust T_i exerted by each actuator is a function of V_{ai} , the relative inlet speed of the fluid and of n_i , the propeller rotational speed. Both rear propellers and thrusters have been assembled in the MDM Lab laboratories: they have been tested and identified in a swimming pool where the bollard thrust of the propeller was evaluated and identified using the experimental layout displayed in Figure 7. Knowing the bollard thrust and the main data of the tested profile, such as the p/d ratio between propeller pass p and diameter d , it is possible to extrapolate for both thrusters and rear propellers a surface, representing the exerted thrust T_i as a tabulated function of the rotation and advance speed n_i and V_{ai} , as reported in Figure 8.

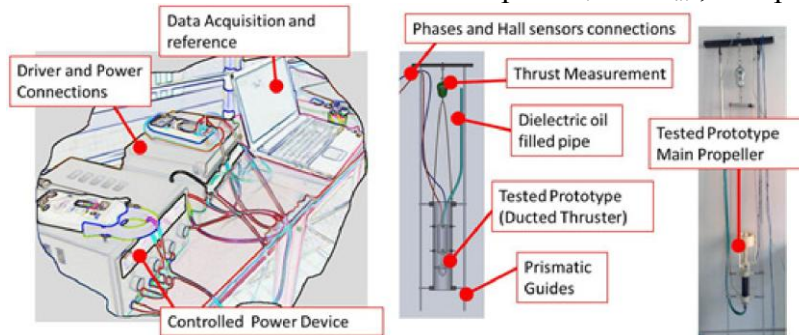


Figure 7: Experimental layout used for the propeller testing

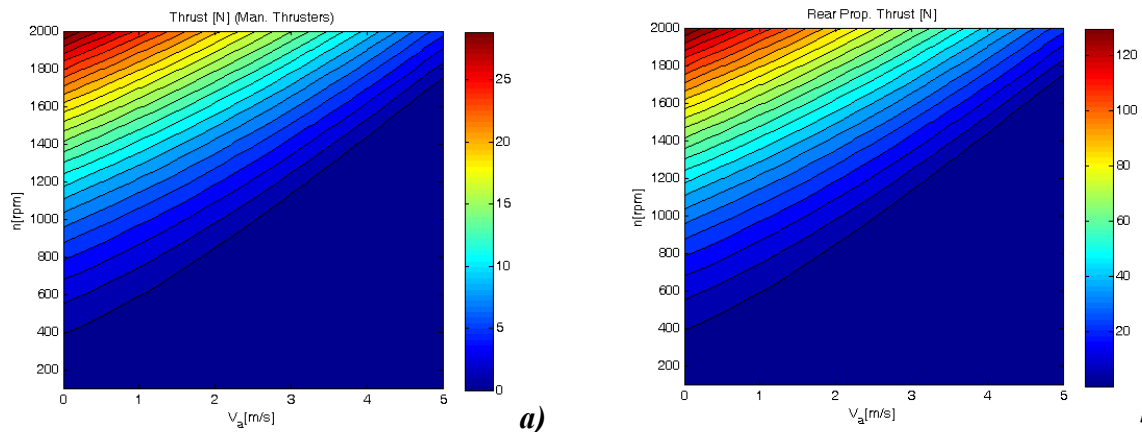


Figure 8: Thruster a) and Rear Propeller b) thrust as a function of propeller rotational and advance speed (V_a , n), obtained from bollard thrust tests performed in MDM Lab pool of Pistoia (Italy)

The six actuators are supposed to be speed controlled since on Tifone vehicle the chosen PM brushless motors are controlled by a drive which support both current (torque) and speed regulations. A speed loop for motors is chosen mainly for two reasons:

- Both motors and thrusters are sized for maximum performance specifications: during low speed, hovering and precision manoeuvring, the propellers have to exert low efforts at quite low speed with respect to the friction of seals and bearing. In order to avoid a friction influenced cogging behaviour of the thrusters and to avoid parametric uncertainties on low amplitude response of the actuator, speed control was preferred.
- Especially for the rear main propellers an assigned propeller speed roughly corresponds to a known advance speed in steady-state conditions. As consequence, a speed controlled propeller can be more advisable for a precise advance speed control of the vehicle.

To control the vehicle (control the desired vehicle pose η_d starting from the pose estimation η_m) a multi-axis regulator is implemented [8] using five PID type-SISO controllers, each one designed to manage a single DOF of the vehicle, as shown in the scheme of Figure 9. This consideration implies that the extra-diagonal terms of the matrices K_P , K_D and K_I of the PID control law (3) are null, since mutual-cross influences among the controlled axis are neglected.

$$\tau_d = K_P e_r + K_D \dot{e}_r + K_I \int_0^t e dt + g_{rb}(\eta) \quad (3)$$

where $e_r = \eta_d - \eta_m$

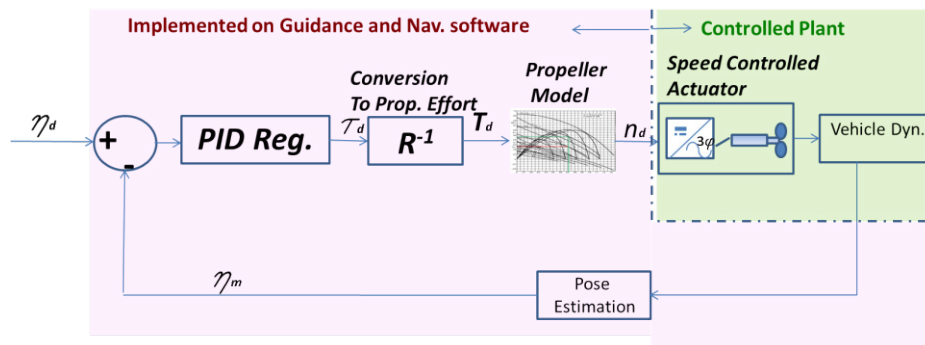


Figure 9: Vehicle control, main components

In (3) it is worth to note the optional feed-forward term $g_{rb}(\eta)$ introduced in order to compensate gravitational and buoyancy contribution.

The output of the regulator is the request of a reference τ_d that have to be converted in reference command for the speed controlled actuators of the propellers. The conversion between the desired effort on the vehicle τ_d and the corresponding speed of propellers is performed using a two stage conversion: first of all, τ_d is converted in the corresponding vector T_d , whose scalar components are the thrust values that have to be exerted by the actuators. Then, from T_d it is possible to evaluate the corresponding desired rotating speeds of each propeller n_d which are used as reference command by the propeller drive system.

Modelling the propeller involves the knowledge of the inlet fluid speed V_a , that, for simulation purposes, was considered as perfectly known/estimated. Since this hypothesis is quite difficult to be verified in real applications, the authors have also considered the case in

which the delivered thrust is roughly estimated as proportional to squared value of propeller speed, through a constant coefficient identified from the bollard thrust experimental tests. In order to further reduce the energy consumption of the vehicle, in parallel with the regulator described by (3) a static-low bandwidth pitch control is implemented, acting on the longitudinal position of batteries along the hull: the position of vehicle centre of mass can be regulated, limiting the use of manoeuvring thrusters and, consequently, the energy consumption. The related mechanical and implementation schemes are respectively shown in Figure 10 and Figure 11.

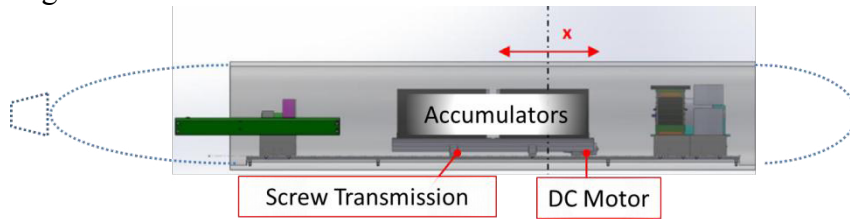


Figure 10: Screw transmission system used to regulate the position of the accumulators and consequently the vehicle center of mass

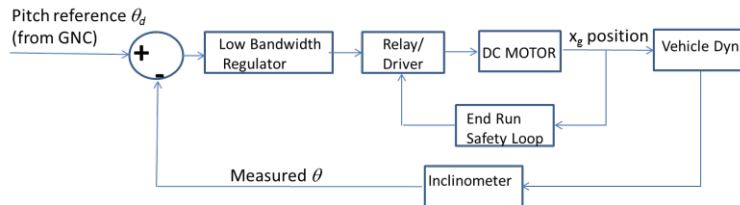


Figure 11: Low frequency pitch control based on the longitudinal translation of batteries

Finally, since one of the main aim of the model was to calculate the energy consumption and conversely to verify the mission autonomy, in the simulation environment the total power consumption W_{tot} is calculated as the sum of elementary contributions W_i of each component, being the i the index corresponding to the i -th component or subsystem:

$$W_{tot} = \sum_{i=1}^n W_i \quad (4)$$

In particular W_i contributions associated to the propellers are calculated from tabulated functions of the propeller rotation and advance speed which have been extrapolated from experimental activities in the MDM Lab pool. For other components, such as sensors or computers, the related consumptions are evaluated in terms of functional states such as *component switched off*, *idle* or *fully working* to which an energy consumption is assigned according to their technical documentation (and verified through the preliminary laboratory activities).

3 PRELIMINARY SIMULATION AND VERIFICATION OF PROPULSION AND ENERGY STORAGE SYSTEM

Using the previously described model it was possible to simulate close to realistic mission profiles, in which the corresponding energy consumptions have been verified, as in the example of Figure 12, where a simple zig-zag path following is represented.

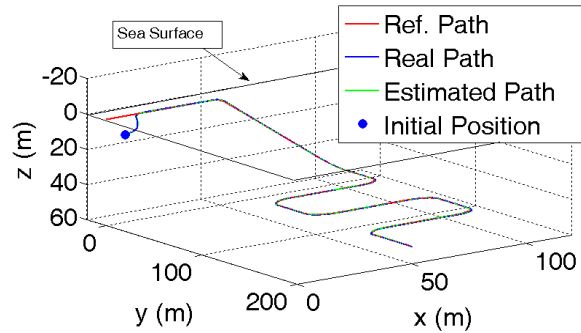


Figure 12 Example of the simulation of a short range mission [8]

Since the simulation of a complete mission of 8-12 hours could be quite heavy in terms of computational resources, the following approach was applied:

- Compiled/not interpreted code: all the simulation code was written in order to support compilation for a generic fast simulation target (e.g. rsim.tlc / matlab rapid simulation target); in this way it is possible to greatly increase the efficiency of the code, also considering simulations of thousands of seconds of equivalent time.
- Assembling of Simple Simulation Scenarios: the simulation of complex operative scenarios was divided in a population of shorter and simple case studies, that were used to calculate the mean consumption profiles associated to each specific task. In this way it is possible to evaluate the mission consumption as a time weighted mean of individual consumption profiles, previously established and calculated. As regards the worst case conditions, related to exceptional power demands, some results are shown in Figure 13.

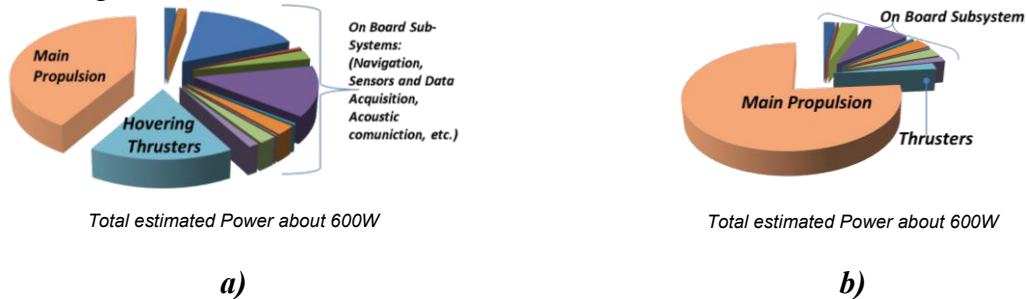


Figure 13: Simulated energy consumptions with worst condition scenarios, such as exploration and hovering on a site with a 1.5 knots current disturbance (a) or fast transfer at maximum speed to an interesting site (b)

It is also possible to evaluate a penalty map in terms of power demand W_e with respect to the cubic value of the advance speed V_a , useful for many future feasible purposes, e.g. optimization of vehicle control strategies. Moreover, considering pure translations of the vehicle, it is possible to calculate the value of the optimal advance speed v_{opt} with respect to traveling direction, which maximizes the vehicle autonomy to the travelled distance, considering a fixed cautious power consumption of the installed components of about 200 W. The results shown in Figure 14 and Figure 15 have been obtained under the hypothesis that the thrusters have a behaviour which is not dependent from their rotation sense; this

hypothesis is almost true for maneuvering thrusters since they adopt a symmetric blade propellers which were optimized for this purpose during the experimental activities. Concerning the main rear propellers, the behaviour in both sense of rotation was also verified with the experimental tests in the MDM Lab pool confirming their asymmetric behaviour, due to blade profiles and to the applied accelerating nozzle (19-A).

Even considering the asymmetric behaviour of the rear propellers the obtained results are quite symmetric with respect to the ordinate axis, since the shape of the obtained functions seem to be more influenced by the corresponding distribution of the hydrodynamic resistances.

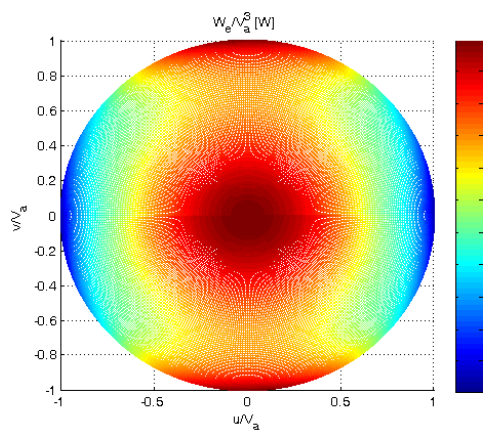


Figure 14: Distribution of the required electric power with respect to the cube of the advance speed considering pure translations

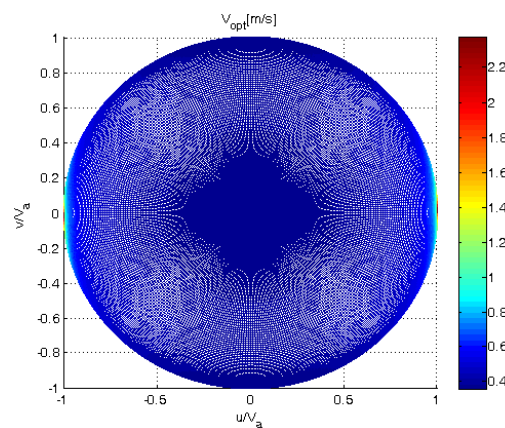


Figure 15: Calculated value of v_{opt} maximizing the vehicle autonomy with respect to travelling direction

From the simulation results it is possible to verify the correct sizing of both the propulsion and energy storage systems, which is composed by two Li-Po accumulators, each one able to deliver 40Ah of DC currents at 48V for a total stored energy of about 4kWh (suitable to largely satisfy the autonomy and speed specifications described in Table 2).

CONCLUSIONS

In this paper some preliminary simulation and testing activities concerning the design of an Autonomous Underwater Vehicle, briefly called Tifone, for the Thesaurus project, are described. Since the vehicle has been successfully assembled, the preliminary testing activities have started at Roffia lake (San Miniato, Pisa, Italy, Figure 16).

The preliminary results are quite encouraging: in particular, the functionality of guidance and navigation systems have been successfully debugged, making possible the execution of simplified mission profiles, including acoustic communication and localization.

The next testing activities will mainly deal with an improved identification of vehicle performances, scheduled for the month of April 2013.



Figure 16: Tifone vehicle during its preliminary testing activities in the basin of Roffia (San Minato, Pisa February 2013) working both as AUV (Autonomous Underwater Vehicle) and ROV (Remotely Operated Vehicle)

ACKNOWLEDGMENTS

The object of this work is within the framework of the Thesaurus Project (<http://thesaurus.isti.cnr.it/>) which has been financed by Regione Toscana as part of PAR FAS REGIONE TOSCANA Linea di Azione 1.1.a.3.

The authors wish to thank all the partners of the project and in particular Professor Andrea Caiti. Finally for the active support in manufacturing and testing the authors want to remember Vito Balducci (Technowave Srl, the manufacturer of most of the structural parts) and the people of CMRE (Centre for Maritime Research and Experimentation) both sited in la Spezia, Italy.

REFERENCES

- [1] Allotta B., Pugi L., Costanzi R., Vettori G., Localization algorithm for a fleet of three AUVs by INS, DVL and Range measurements, The 15th International Conference On Advanced Robotics , Tallinn, June 20-23 2011.
- [2] Cairns J., Larnicol E., Ananthakrishnan P., Smith S., Dunn S., Design of AUV propeller based on a blade element method, OCEANS '98 Conference Proceedings , pp. 672-675, vol.2, 1998.
- [3] The Oxford robotic group, The Mission Oriented Operating Suite, (doc. available on line).
- [4] T.I. Fossen, Guidance and Control of Ocean Vehicles, 1^o Edition , UK: John Wiley and Sons 1994.
- [5] Xianzhao Yu, Yumin Su, Hydrodynamic performance calculation on mini-automatic underwater vehicle, Proceedings of the 2010 IEEE International Conference on Information and Automation June 20 - 23, Harbin, China.
- [6] P. Jagadeesh, K. Murali, V.G. Idichandy, Experimental investigation of hydrodynamic force coefficients over AUV hull form, Journal of Ocean Engineering 36, pp. 113–118, 2009.
- [7] Peter Michael Ostafichuck, AUV Hydrodynamics and modelling for improved control, PhD Thesis at University of British Columbia, 1997.

- [8] B. Allotta, R. Costanzi, N. Monni, L. Pugi, A. Ridolfi and G. Vettori, Design and Simulation of an Autonomous Underwater Vehicle, European Congress on Computational Methods in Applied Sciences and Engineering, ECCOMAS 2012, Vienna, Austria, September 10-14, 2012.
- [9] Caffaz A., Caiti A., Casalino G., Turetta A., The Hybrid Glider-AUV Folaga, Robotics and Automation Magazine IEEE , Vol. 17, Issue 1, March 2010.